TESTING OF A NOVEL NITROUS-OXIDE AND ETHANOL FUEL BLEND

BARCELO RENACIMIENTO HOTEL, SEVILLE, SPAIN / 14 - 18 MAY 2018

Iain Waugh[1,2], Ed Moore[1], James Macfarlane[1], Adam Watts[3], and Alfons Mayer[4]

[1] *Airborne Engineering Ltd., Westcott Venture Park, Aylesbury, HP18 0XB, UK*
[2] *Corresponding author: iain@ael.co.uk*
[3] *Nammo Westcott, Westcott Venture Park, Aylesbury, HP18 0NZ, UK*
[4] *TNO Defence, Security and Safety, P.O. Box 45, 2280 AA Rijswijk, The Netherlands*

KEYWORDS:

Nitrous oxide, fuel blend, green propellant

ABSTRACT:

As part of a global drive to move towards less toxic propellants, Nitrous Oxide Fuel Blends (NOFB) have been identified as a potential monopropellant to replace hydrazine. The European Fuel Blend Development programme was initiated as a low TRL investigation to further develop European knowledge and capability in this area. TNO undertook a scoping study to downselect to a promising fuel blend of nitrous oxide and ethanol, and performed initial miscibility studies. This fuel blend was then tested with hot firings.

This paper describes the test rig design for mixing and injecting the liquid NOFB, and presents initial results from the first hot-firings. The NOFB was found to have good combustion efficiency and performance. No flashback events were seen with the current setup. Two downsides were noted, however: first, that the pre-mixed propellant was found to burn quickly with high heat release, resulting in large heat loss to the copper combustion chamber, and injector face burnout in the final test. Second, that the injector pressure drop was found to be strongly dependent on the temperature of the injector face, because the heat transfer increases the proportion of nitrous oxide that flash boils in the injectors.

1. INTRODUCTION

There is currently a global drive to move towards less toxic propellants, with a particular focus on replacing hydrazine as a monopropellant. Hydrazine has historically been the dominant propellant for in-space propulsion because of its high specific impulse, storability and because it can operate as a monopropellant with a suitable catalyst. It is extremely carcinogenic, however, and therefore requires complex procedures for safe handling by personnel and requires safe disposal. It is considered a substance of very high concern (SVHC) under the EU REACH regulations, and the future of its use in Europe is therefore uncertain.

There are several “green propellants” currently being investigated as potential low-toxicity replacements for hydrazine. The most promising propellants include those based on ammonium dinitramide (ADN), hydroxyl ammonium nitrate (HAN) and concetrated hydrogen peroxide. ADN based propellants such as LMP-103S developed by ECAPS have been shown to have higher specific impulse and density impulse than hydrazine and have been demonstrated in space over 5 years on the PRISMA satellite [2]. HAN propellants, such as AF-M315E, have an even higher density impulse (45% higher than hydrazine) and have also been tested in space on the GPIM technology demonstration mission [3]. Hydrogen peroxide has a much lower combustion temperature than the other propellants, which reduces thermal load onto the combustion chamber, but has a lower specific impulse than hydrazine. It has been used in many sea level applications, but is not currently used widely for in-space thrusters.

Nitrous Oxide Fuel Blends (NOFB) have also been identified as a potential monopropellant to replace hydrazine. Nitrous oxide is a good solvent and stable oxidiser. The fuel blends consist of a hydrocarbon fuel mixed with nitrous oxide, to form a monopropellant. NOFB have the advantages of the high performance of a bipropellant, with the self-pressurising nature of

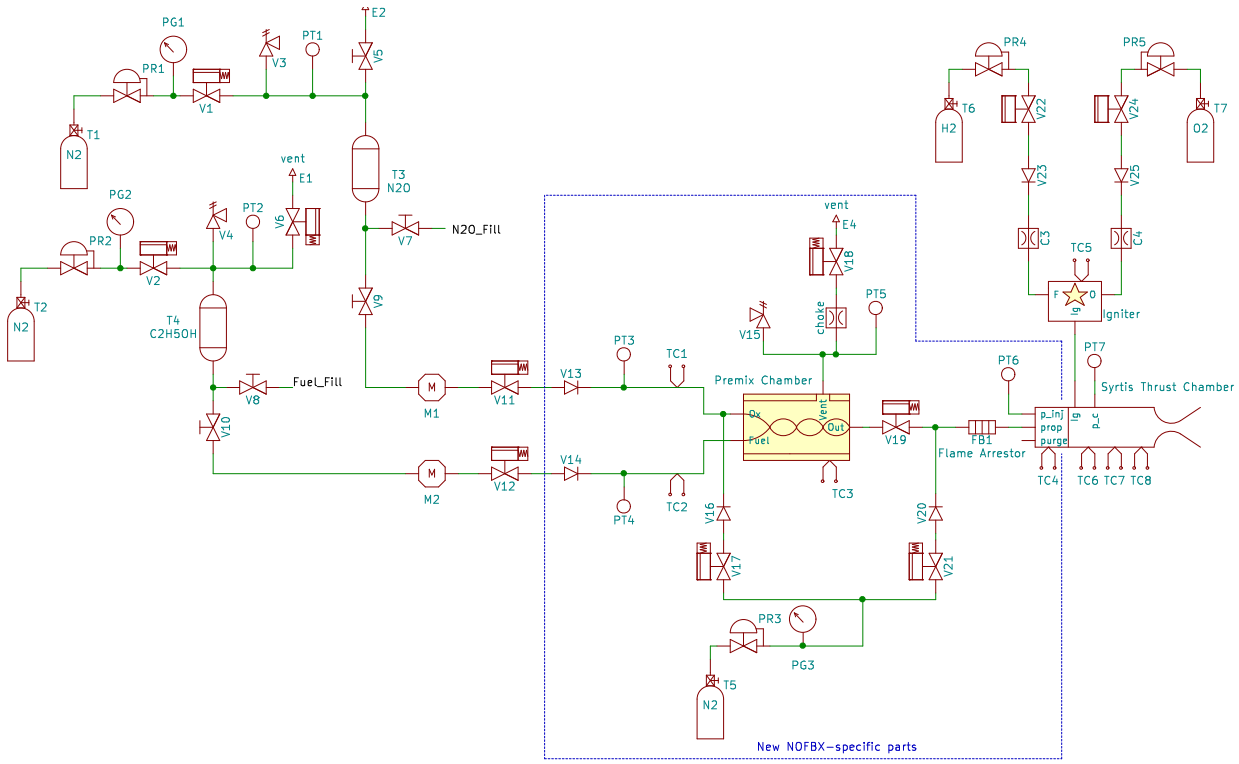

Figure 1: Process and instrumentation diagram for the NOFB test rig.

the nitrous oxide, meaning that a separate pressurant supply is not required which greatly reduces plumbing complexity and weight. However, NOFB have the disadvantages of the high combustion temperatures of a bipropellant, the phase changes of a self-pressurising propellant, and the inherent danger of flame flashback into the plumbing system.

Early work on NOFB was undertaken in the US by Firestar Technologies LLC who patented the "NOFBX" propellant, developed several thruster concepts and tested the propellant handling qualities [1]. Much of the European research into NOFB has been conducted by DLR at Lampoldshausen, who have used ethene for their "HyNOx" propellant formulation because it has a similar vapour pressure to nitrous oxide. They have designed a test rig for gaseous propellants [4], tested components for flashback arrestors [6], demonstrated the performance of the propellants in hot firings [5, 8] and back-calculated the heat flux in the combustion chamber [7]. Initial results have been promising from a performance perspective.

1.1. European Fuel Blend Development programme

The European Fuel Blend Development programme was initiated as a low TRL investigation to further develop European knowledge and capability in this area. TNO undertook a scoping study to select to a promising fuel blend of nitrous oxide and ethanol, and performed initial miscibility studies, described in detail in [9]. TNO partnered with Nammo Westcott to organise the test programme, who selected Airborne Engineering Limited (AEL) to undertake the hot-fire testing of this propellant at the AEL test site in Westcott, UK. The test programme used an existing combustion chamber and a modified test rig to hot-fire a nitrous oxide/ethanol fuel blend at several O/F ratios around the target operating condition (O/F 3.18), chosen based on the outcomes from the scoping study by TNO. The test programme was overseen by TNO and representatives from ESA, with funding from the ARTES 5.1 programme.

This paper describes the test rig design for mixing and injecting the NOFB, and presents initial results from the first hot-firings.

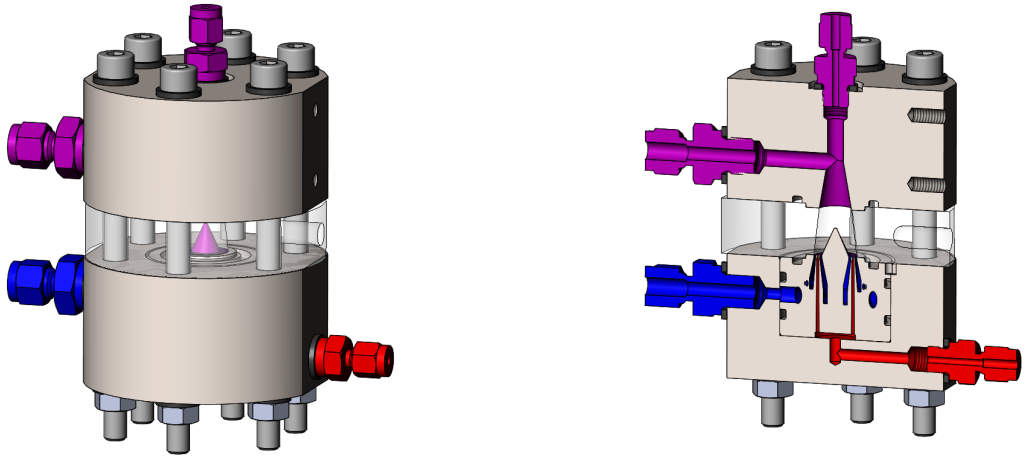

(a) Outer surface *(b) Cross section*

Figure 2: Pre-mix chamber consisting of four machined parts: the additively manufactured injector block and injector housing, the chamber outlet and the chamber spacer (acrylic). The flow paths are colour coded dependent on the fluid: fuel (red), oxidiser (blue), NOFB (purple). There are two outlets, one to the engine (horizontal), and one to a choke which was sized to maintain steady state backpressure during filling (vertical).

2. TEST RIG

The handling properties of the chosen ethanol NOFB are largely unknown. It was therefore considered too dangerous to use a pre-mixed tank of the fuel blend for the hot-firing tests, because of the risk of flashback through the plumbing. It was therefore decided to use a standard bi-propellant setup with two separate feed systems and to mix the propellant in real time in a small volume just before injection into the combustion chamber. Furthermore, it was decided to maintain the propellant in a liquid form up until the point of injection, because there will then be a high degree of flash-boiling during injection, and therefore good isolation between the plumbing and the combustion chamber.

Fig. 1 shows a simplified P&ID for the test rig. Both propellant tanks are pressurised with nitrogen with appropriate valves for pressure relief, isolation, fill and drain. The propellants pass through separate coriolis mass flow meters before passing into a small pre-mix chamber, before then passing through a run valve and a flashback arrestor made from sintered stainless steel. A nitrogen purge system purges both the pre-mix chamber and the injector gallery immediately after test completion. A hydrogen-oxygen gas torch igniter was used.

2.1. Pre-mix chamber

The purpose of the pre-mix chamber is to mix the two propellants in real time, in their liquid state, before they are fed to the engine's injector. This is to avoid any hazards associated with mixing and storage of the fuel blend. The pre-mix chamber must form a homogenous NOFB liquid, and must have a minimal volume of pre-mixed propellant, although significant in comparison to the injector volume in order to minimise flash boiling when the run valve is opened.

The pre-mix chamber must therefore mix the two liquids efficiently in a small volume. At high Reynolds number, liquid mixing from a jet occurs from turbulent dissipation of structures, commonly either from jet impingement or from vortical rollup at a liquid-liquid shear layer. For the NOFB pre-mix chamber, it is important that there is very little unused volume to minimise stored energy. Unused volume is common for jet impingement injectors, where the jets commonly form only part of the area of a larger face. For the NOFB project there is also a large difference in volume flow rate between the two liquids - it is dominated by the nitrous oxide flow. This has two effects: first, it makes distribution of the fuel the priority for mixing, and second, it means that the bulk of the turbulence generation has to come from the larger nitrous oxide flow.

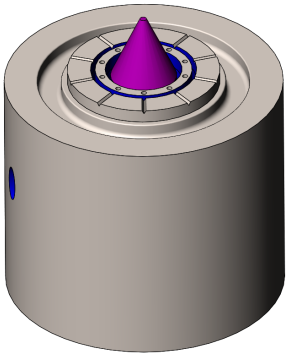

(a) As printed

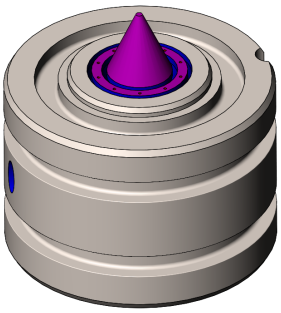

(b) Post-machined

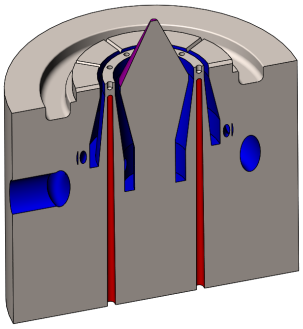

(c) As printed cross section

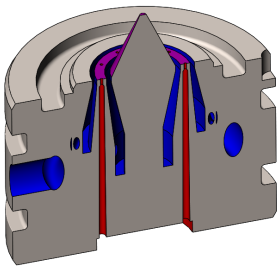

(d) Post-machined cross section

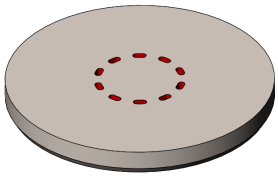

(e) Fuel passageways

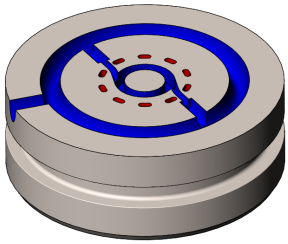

(f) Oxidiser gallery and inner swirl gallery

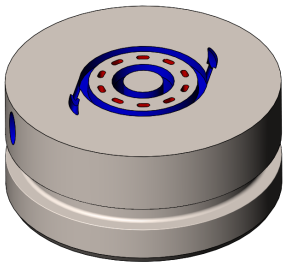

(g) Oxidiser outer swirl gallery

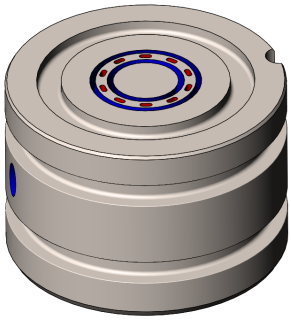

(h) Galleries before final injection

Figure 3: Pre-mix injector block, showing as printed ((a),(c)) and post-machined geometry, including cross sections showing the internal manifolding. The flow paths are colour coded dependent on the fluid: fuel (red), oxidiser (blue), NOFB (purple).

The pre-mix chamber was therefore designed to mix the ethanol into the nitrous oxide as homegenously as possible, whilst minimising the unused chamber volume by using almost the entire injector face. To achieve this, the pre-mix injector:

1. Splits the nitrous oxide into two swirling flows.
2. Generates a strong shear layer using the two contra-rotating nitrous oxide flows to maximise turbulence.
3. Pre-distributes the fuel using plumbing as much as is reasonably practical.
4. Injects the small fuel flow rate directly into the nitrous oxide shear layer to maximise its distribution by the turbulence.

Fig. 2 and 3 show the geometry of the pre-mix chamber and the additively manufactured pre-mix injector. All parts are made from aluminium except the acrylic chamber spacer.

The pre-mix chamber features a vent connection on the top. This allows gas to be purged from the pre-mix chamber before firing. Furthermore, the vent allows the pre-mix chamber to be filled with fuel blend ahead of the firing. This is achieved by a metering choke fitted into the vent line which gives an equivalent back-pressure to that of the main injector / engine. The clear acrylic spacer allows verification of the flow phase in the pre-mix chamber and also provides a deliberate failure zone to deal with over-pressure events.

The pre-mix chamber injector involves two counter-rotating swirling flows of oxidant, each roughly half the mass flow, with the fuel injected in axially through ten 0.5mm holes at the shear layer between the swirling flows. The mixing therefore occurs due to the shear between the ±40m/s counter-rotating flows in the tangential direction, and the shear between the ~40m/s fuel jet and slow moving oxidiser flows in the axial direction. The swirling of the oxidant was achieved through tangential holes into galleries, and the injection of the fuel through small axial holes distributed evenly around the circumference between the two swirling flows. A centrebody reduces the chamber volume whilst keeping the shear layers together. A significant pressure drop exists between the individual fuel and oxidiser feeds in order to provide sufficient hydraulic isolation of the feed systems.

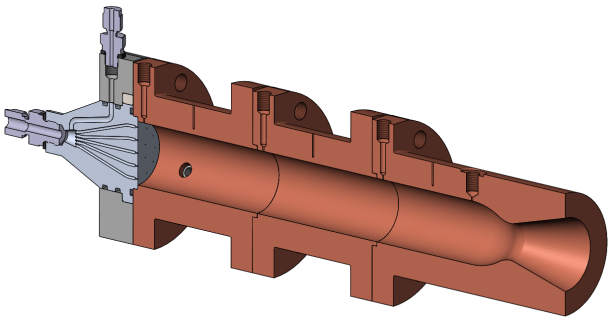

Figure 4: Section of the 3D printed aluminium injector block and copper heat sink combustion chamber as used in the NOFB tests.

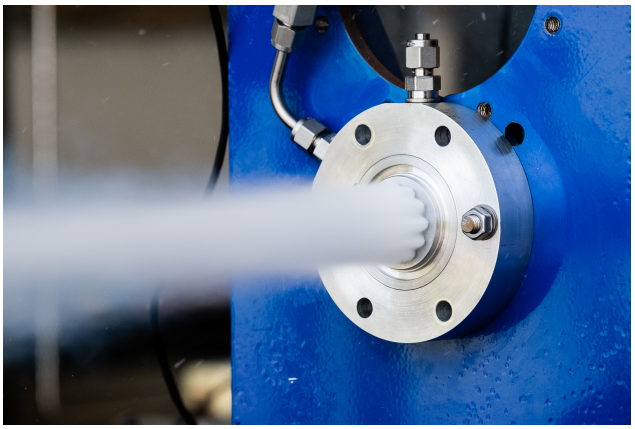

Figure 5: Flash-boiling of the NOFB from the showerhead injector in a cold flow test without combustion chamber.

2.2. Monopropellant Injector

The injector for the combustion chamber was a simple showerhead because there is no need for mixing within the combustion chamber. The injector has 19 holes. The injector holes are each fed by its own internal pathway of approximately 1.5mm diameter and 50mm long, in order to reduce dribble volume of pre-mixed propellant. There is a high pressure drop across the injector to keep the nitrous oxide in the liquid state in the pre-mix chamber. This means that there will be a significant amount of flash-boiling in the injector orifices. This flash-boiling should help keep the flame front within the combustion chamber.

Nitrous oxide injector flash-boiling is a complicated process, which relies on the pressure drop, heat load from the injector and stay time in the injector orifice. It has been studied in detail in the literature [11, 12, 10]. The nitrous oxide behaves somewhere between two limits: first, the single phase incompress-

ible (SPI) limit, where the nitrous oxide remains liquid, and second, the homogeneous equilibrium (HEM) limit, where the nitrous oxide remains in equilibrium, expands isentropically and the phases travel at the same velocity. The model proposed by [11], with a correction by [12] and tested by [10] uses a smooth blending between the SPI and HEM extremes, based on the relative bubble growth time and residence time in the injector. This model is known as the Non-Homogeneous Non-Equilibrium (NHNE) model [10], and has been tested extensively for cold flow injection at a range of injector and chamber pressures.

The NHNE model was used to calculate the injector hole sizes for the showerhead injector. Fig. 4 shows the injector block. It was additively manufactured from aluminium and post-machined on the sealing surfaces and drilled on the injector face. Aluminium was used for its relatively high thermal conductivity and because it decomposes nitrous oxide less than copper at high temperature. Because the injector was only used for very short firings, its lower melting temperature was considered sufficient given experience with previous bipropellant injectors. Fig. 5 shows the flash-boiling of the fuel blend in cold flow testing without the combustion chamber. The experimental cold flow injector pressure drop results matched well with those predicted by the theoretical NHNE model [10].

3. CHARACTERISTIC VELOCITY

The characteristic velocity, c^*, is often used to categorise the combustion in the chamber, because it is independent of the nozzle geometry. Some calculation steps are required, however, to accurately compare experimental c^* values, based on static pressure measurements, and theoretical c^* values once heat loss to the combustion chamber is taken into account. As will be shown in the results section, this heat loss is particularly important for NOFB propellants.

The experimental c^* value is calculated as:

$$c^* = \frac{p_{eoc,0} A_t}{\dot{m}_{TOT}} \tag{1}$$

where the throat area is based on a measured diameter of 21.05mm (A_t = 3.48$\times 10^{-4}$m^2). No adjustment of throat area is made for the temperature of the nozzle during hot firing, because this requires significant FEA analysis and thermal measurements and was therefore out of scope of this programme.

The static chamber pressure, p_{eoc}, is measured at the end of the combustion chamber (eoc). The chamber stagnation pressure, $p_{eoc,0}$ can be found from this using the ratio of specific heats, γ_{eoc}, and the chamber Mach number, M_{eoc}, which is a function of the combustion chamber to throat area ratio. Both M_{eoc} and γ_{eoc} are found from CEA [13].

$$p_{eoc,0} = p_{eoc} \left(1 + \frac{\gamma_{eoc} - 1}{2} M_{eoc}^2\right)^{\frac{\gamma_{eoc}}{\gamma_{eoc}-1}} \tag{2}$$

3.1. Heat loss rate

Heat is lost from the combusting gasses to the copper heat sink chamber and the aluminium injector head. Calculating the heat flux as a function of position in the chamber is a complex problem and for good fidelity requires many thermocouples, or coolant calorimetry, and as such it cannot be done with the current experimental setup.

The average heat loss to the chamber can be calculated, however, by calculating the total enthalpy rise in the chamber components using calorimetry and then dividing by the run time. This average value will be fairly accurate when the chamber pressure remains roughly constant during a test.

The average heat loss rate is therefore given by:

$$q_{hl,ave} = \frac{\sum_i m_i c_i \left(T_{end} - T_{start}\right)}{\Delta t} \tag{3}$$

where mc are the thermal mass values of the aluminium injector and copper chamber sections, Δt is the firing time, T_{end} is the temperature at the end of the dataset when the temperatures have equilibrated (at 30s for the hot firings) and T_{start} is the temperature at the start of the firing. The start and end of the firing, which define Δt, are taken as where the chamber pressure has risen above half of its maximum value. The start time is therefore commonly around 0.4s, rather than 0s, which helps ignore additional heat input from the gas torch igniter. By using half the maximum chamber pressure as the threshold, the firing time takes account of the ramp-up and ramp-down times of the chamber pressure (and therefore ramping of the heat flux to the combustion chamber); this should produce a better 'average' heat loss rate from the calorimetry, because the average assumes that the heat load is constant with time.

3.2. Theoretical characteristic velocity

The theoretical characteristic velocity, c^*_{theor}, is calculated by the CEA program [13] using a multiple pass process. In all cases the finite area combustion model is used, with the experimental combustion chamber area to throat area ratio (3.07). Using the finite area combustion model allows calculation of the combustion chamber Mach number and ratio of specific heats, and also incorporates the stagnation pressure loss due to acceleration of the gases between the injector (inj) and the end of the combustion chamber whilst under heat addition. This is roughly 2% in this case, and can be expressed as a function of the chamber Mach number using Rayleigh flow assumptions and using integrated Mach equations ([14] with typographical correction).

$$\frac{p_{inj,0}}{p_{eoc,0}} = \frac{1+\gamma_{eoc}M^2_{eoc}}{\left(1+\frac{\gamma_{eoc}-1}{2}M^2_{eoc}\right)^{\frac{\gamma_{eoc}}{\gamma_{eoc}-1}}} \tag{4}$$

In all cases equilibrium thermodynamics are assumed in the nozzle, because frozen thermodynamics cannot be used simulatenously in CEA with the finite area combustion model. The c^*_{theor} values for equilibrium thermodynamics will be slightly higher than the frozen flow equivalents, with the real nozzle flow somewhere between the two.

The input enthalpy of the nitrous oxide is specified to CEA using the enthalpy of formation (ΔH_f = +82.05kJ/mol) plus the enthalpy difference between the injection conditions at chamber pressure and premix chamber temperature and those at standard temperature and pressure. Note that the premix chamber temperature, T_{pmx}, must be used here because there was no thermocouple in the injector flow itself. The calculation method used in this paper extremely similar to that used in [8] for analysing "HyNOx" propellants, although the heat loss rate here is calculated by calorimetry. To avoid confusion, the notation used here is similar to [8]. When calculating the heat-loss adjusted characteristic velocity, $c^*_{theor,hl}$, the input enthalpy of nitrous oxide is therefore specified as:

$$\begin{aligned} H_{N2O,hl} = \quad & \Delta H_f + \big(H(p_c, T_{pmx}) - H(10^5, 298.15)\big) \\ & - \tfrac{q_{hl,ave} M_{N2O}}{\dot{m}_{N2O}} \end{aligned} \tag{5}$$

where the molar mass, M_{N2O} = 0.0440123 kg/mol, and massflow of nitrous oxide, $\dot{m}_{N2O}$, are used to convert the enthalpy into kJ/mol for the input to CEA.

This process therefore removes the heat loss enthalpy from the input oxidiser stream. An equivalent could be done for the fuel stream, and both can be shown to result in the correct enthalpy loss from the combusted gases, but the oxidiser is used here for convenience.

The theoretical characteristic velocity values are therefore calculated in three steps:

1. Call CEA with pressure ratio $p_{inj}/p_e = p_{eoc}/p_{atm}$, with exit pressure set to atmospheric, $p_e = p_{atm}$, and H_{N2O} to obtain the ratio of p_{inj}/p_{eoc}.
2. Call CEA again but with the scaled injector pressure $p_{inj}/p_e = p_{inj}/p_{eoc} * p_{eoc}/p_{atm}$. This then matches the static pressure at the end of the combustion chamber to that of the experimental value (technically one should iterate here but the pressure value is close after a single pass). This results in the values for c^*_{theor}, γ_{eoc} and M_{eoc}.
3. Call CEA as before but with the heat loss adjusted oxidiser enthalpy, $H_{N2O,hl}$, to get the value for $c^*_{theor,hl}$.

The combustion efficiency values, η_{c^*}, can then be calculated for the standard and for the heat loss adjusted cases.

$$\eta_{c^*} = \frac{c^*}{c^*_{theor}}\,, \quad \eta_{c^*,hl} = \frac{c^*}{c^*_{theor,hl}} \tag{6}$$

This heat loss adjustment will likely be slightly conservative for two reasons. First, because after the firing some heat transfer will occur from the chamber and injector to the surrounding support structure, pipe work and air, and this enthalpy rise is not accounted for by the calorimetry. Second, because some heat will be lost to the cold nitrogen gas purge. It should be noted, however, that some enthalpy from the torch igniter will be erroneously included in the heat loss calculation due to the cross over time between main propellant flow and igniter flow; this would act to reduce the heat loss adjustment.

4. RESULTS

Reagant grade ethanol (>99.8%) and technical grade nitrous oxide were used to create a liquid NOFB. The liquid NOFB was hot-fire tested at the desired operating condition (O/F 3.18) and two other mixture ratios, one leaner (O/F 3.83) and one richer (O/F 2.21). Unfortunately, the showerhead injector face was eroded after only a few firings, but some key conclusions can be drawn from the available data, albeit without the statistical certainty from repeated test points.

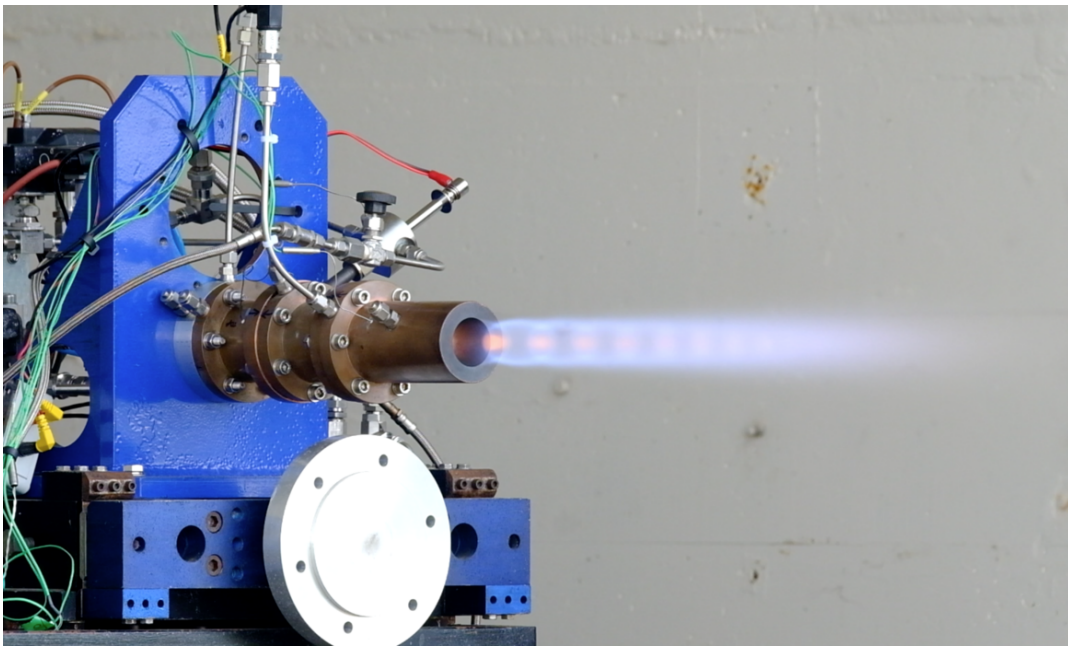

Figure 6: Stable combustion of a liquid nitrous oxide/ethanol fuel blend at mixture ratio 3.85.

4.1. Mixture ratio 3.83

At the leaner condition (O/F 3.83) the propellant lit, burned and shutoff smoothly. A minor combustion instability was visible on the chamber pressure trace, at 25Hz with amplitude 0.1bar (1.4% of chamber pressure). No flashback into the injector gallery was seen on shutdown or startup, which is visible from the smooth injector pressure trace in Fig. 7(b). This suggests that the combination of flash boiling in the injectors, followed by immediate nitrogen purge (visible as the tail Fig. 7(b)) was sufficient for preventing flashback in this test setup.

Table 1 shows key time-averaged values for a test at mixture ratio 3.83. The combustion efficiency of the NOFB was 93.4% when no heat losses are taken into account, but this increases to 97.5% when this is corrected for heat lost to the chamber. Given that the heat loss correction is slightly conservative, this suggests that there was almost complete combustion in the chamber, which in turn suggests a fairly homogeneous propellant mixture; the injector was only a showerhead which has poor mixing between injector flows and therefore could not homogenise the flow if there were large mixture ratio variations between injector elements.

Table 1: Key time-averaged values for mixture ratio 3.83, averaged in the two windows shown in Fig. 7 at times 1.88s and 2.83s. Derived performance values are calculated and compared with theoretical ones calculated with CEA.

	1.88s	**2.83s**	
Injector Feed	63.93	64.83	bar(g)
Chamber	7.54	7.57	bar(g)
Ethanol	0.043	0.043	kg/s
N_2O	0.166	0.166	kg/s
O/F	3.86	3.83	
Total	0.208	0.209	kg/s
Premix Chamber	18.43	18.27	°C
Injector Face	146.64	164.02	°C
c^*_{theor}	1567.5	1566.8	m/s (CEA)
$c^*_{theor,hl}$	1502.2	1501.0	m/s (CEA)
c^*	1460.5	1463.4	m/s (Derived)
η_{c^*}	93.17	93.40	% (Derived)
$\eta_{c^*,hl}$	97.22	97.49	% (Derived)

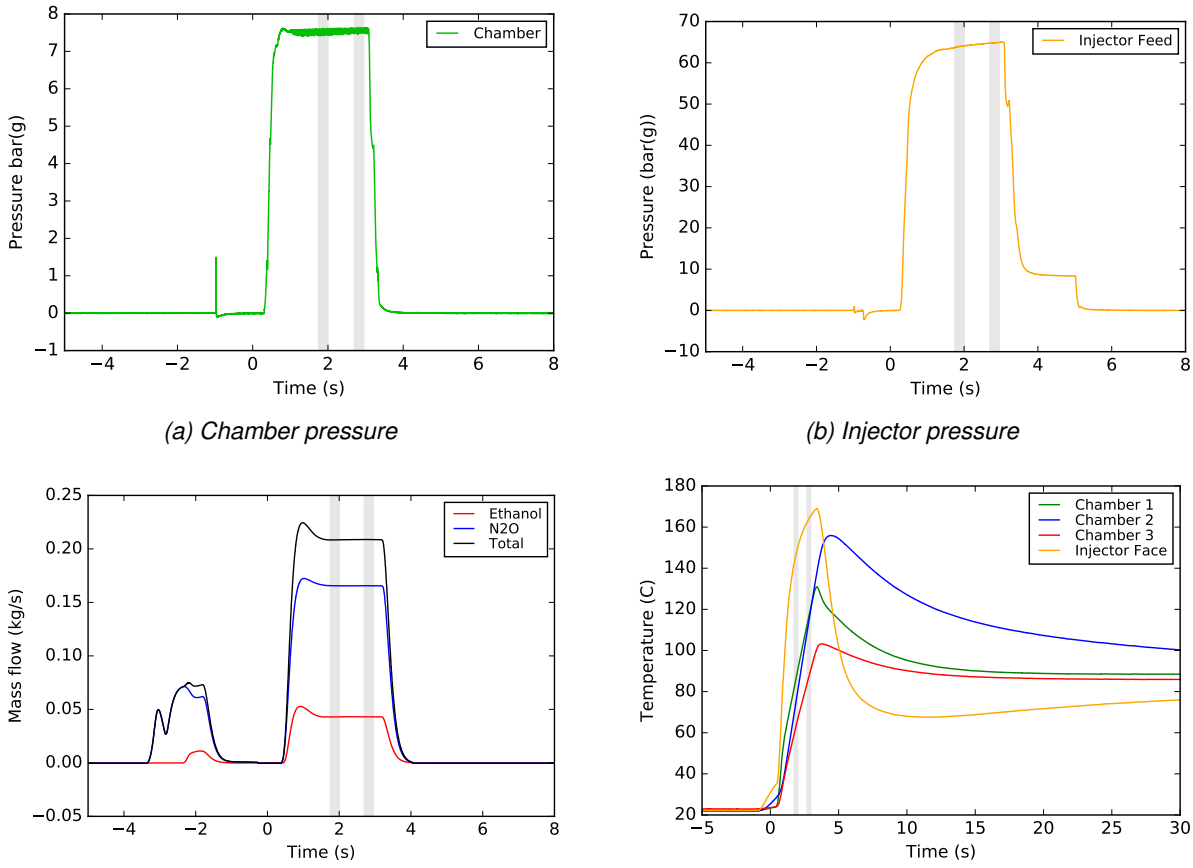

(a) Chamber pressure

(b) Injector pressure

(c) Mass flows

(d) Chamber temperatures

Figure 7: Key traces from the hot firing with liquid NOFB at mixture ratio 3.83. Steady massflow (c) and chamber pressure (a) are achieved after roughly 1.5s, but the injector pressure increases (b) with the injector face temperature (e). The time-averaging windows are shown as vertical grey bars. Note that all graphs have the same time base, apart from the chamber temperatures (in order to show the effect of thermal soak). Time 0s is when the main run valve is commanded to open.

4.2. Mixture ratio 2.21

At the richer mixture ratio of 2.21 the propellant lit, but with rough combustion in the chamber and with significant external burning (Fig. 8(a)), before the flame blew out shortly after the torch igniter was shut off (Fig. 8(b)). Fig. 8(c) shows the resulting chamber pressure trace, which has amplitude fluctuations of 1.5bar at roughly 90Hz. Fig. 8(d) shows the injector pressure trace, which exhibits amplitude fluctuations of up to 0.6bar at the same frequency. Although the propellant did not burn properly, this firing was nonetheless useful as it may provide an insight into the lower flammability limit of the NOFB, indicating it may be between 2.21 and 3.20, with the caveat that only one data point is available here.

4.3. Mixture ratio 3.20

At the design operating condition (O/F 3.20 - target 3.18 [9]) the NOFB lit well with smooth combustion. The injector pressure climbed during the test more steeply than at a mixture ratio of 3.83, however, and the injector face temperature rose more quickly. The injector face melted at the very end of the firing, when sparks were noticed coming from the exhaust. Fig. 9 shows images from the firing. A colour change in the exhaust can be noticed at 2.35s, and sparks by shutdown at 3.1s. The redline (automatic shut-off threshold) specified for maximum injector face temperature was 250°C. At propellant valve shutdown, the measured injector face temperature was 245°C, so the redline wasn't exceeded, but with thermal soak the temperature reached 272°C.

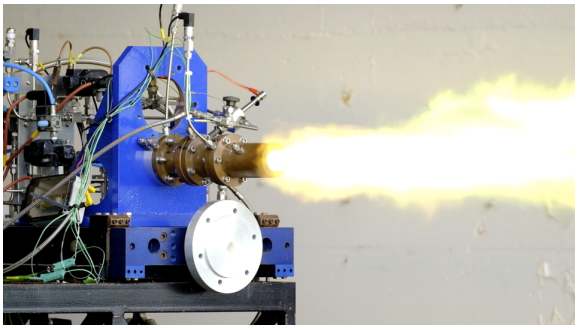

(a) Rough combustion with external burning (0.71s)

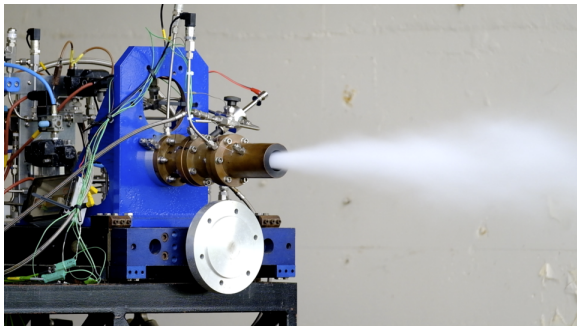

(b) Flameout after igniter stopped (1.75s)

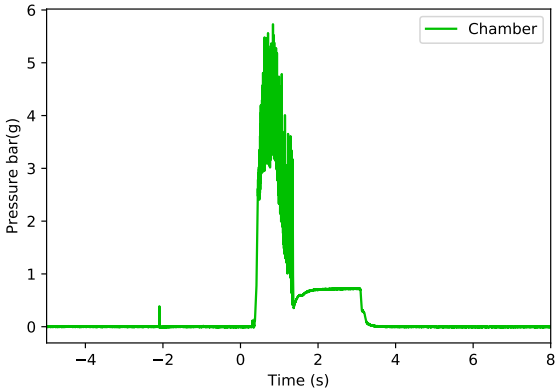

(c) Chamber pressure

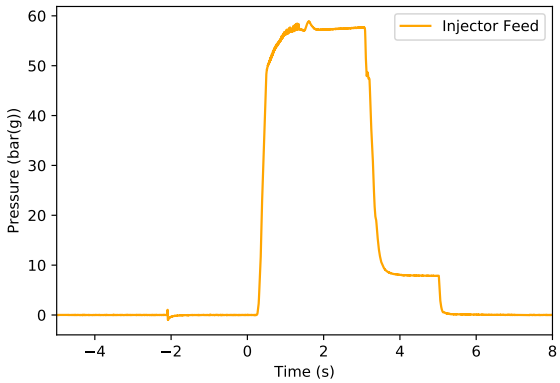

(d) Injector pressure

Figure 8: Data from a fuel rich NOFB test (O/F 2.21). The propellant lit roughly whilst the igniter was running, with significant external burning (a), but the flame blew out shortly after the torch igniter was shut off (b). The rough combustion is seen from the chamber pressure trace (c), and some oscillation on the feed pressure trace (d).

These measurement values were significantly less than the melting temperature of the injector at ~660°C, suggesting that there was a large thermal gradient between the injector face thermocouple and the injector face and therefore a large heat flux from the combusting propellant. For future propellant testing, the thermocouple should be mounted closer to the injector face, and either a protective coating applied or water cooling paths printed into the part. Similar injector materials have been used successfully on the same test rig with the propellants in a bipropellant configuration, which shows that the injector heat flux was significantly higher for the pre-mixed NOFB.

4.4. Heat loss to the chamber

The heat loss correction accounts for 4.1% of the total c^* at mixture ratio 3.83 and 5.8% at mixture ratio 3.20. This suggests that the heat sink combustion chamber was overly long for the current NOFB tests. For other propellant and injector combinations tested previously on this copper chamber, the heat lost to the combustion chamber walls has been lower, commonly one or two per cent. The increase of heat loss makes physical sense for a pre-mixed propellant and a showerhead injector, because the NOFB propellant requires no “mixing distance” and therefore burns early in the chamber, and because there is no protective boundary layer of unburnt propellant near the chamber walls (such as occurs with coaxial injectors).

The large heat loss correlates well with the experimental data for the “HyNOx” propellant [8]. Those experiments examined the effect of the chamber L^* on the heat lost to a variable length copper heat-sink chamber and therefore the effect on combustion efficiency, and showed that the combustion efficiency drops quickly as a function of L^*. At the L^* value used in the current programme (0.83m), η_{c^*} ~ 0.935 [8], which is comparable to the 4.1-5.9% loss in the current programme.

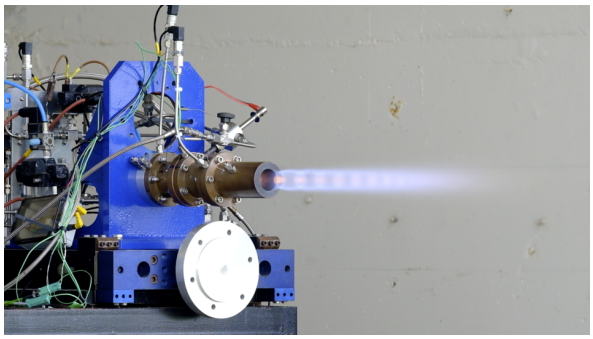

(a) Stable combustion (1.8s)

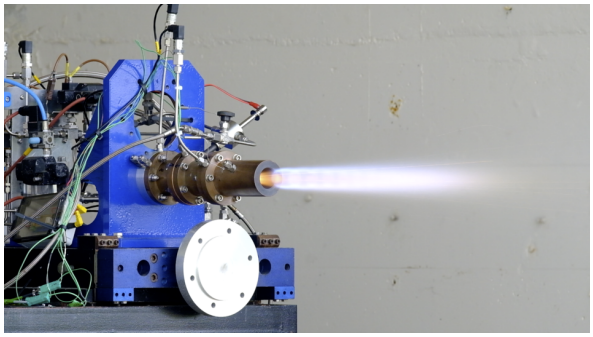

(b) Injector beginning to melt (2.35s)

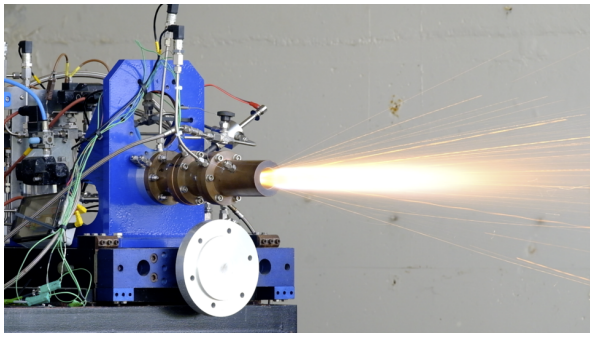

(c) Injector melting (3.05s)

Figure 9: Stable combustion at mixture ratio 3.20, but with melting of the 3D printed aluminium injector face. The melting was first noticed as a colour change of the exhaust in the throat region (b), followed by sparks in the exhaust (c).

4.5. Injector flash boiling

The NHNE method predicts that a rise in chamber pressure has smaller effect on the injector pressure, because the injectors are "choked" by the flash-boiling [10]. This was not seen in the hot flow results, however, where the injector pressure actually increases more than the chamber pressure increases.

Fig. 7(b) shows that the injector pressure continuously increases during the firing, but the massflow, chamber pressure and feed temperatures do not. The injector face temperature does continuously increase during the firing, however. The NHNE method is very sensitive to the temperature when close to the saturation line, so if there is any heat flux to the propellant during injection a higher pressure drop is required for any given massflow.

The effect of injector face temperature on the flash-boiling can be shown by comparing the effective discharge area of the injectors ($\mathrm{C_dA}$); the true value measured from water calibration tests is compared with calculated values using the SPI and NHNE methods [10]. There was no temperature sensor in the propellant flow directly before the injector face, so the NOFB temperature is assumed to be at the measured premix chamber temperature for calculating fluid properties. For both the SPI and NHNE methods, the nitrous oxide and ethanol are assumed to act independently, and the calculated $\mathrm{C_dA}$ values are added together. In both cases the ethanol is assumed to remain liquid and therefore uses the SPI equation.

Fig. 10 shows the estimated effective discharge area of the injectors ($\mathrm{C_dA}$) using time-averaged data, plotted against the injector face temperature. It demonstrates several things. First, that the NHNE equation works well when the injector face is cold, because the calculated $\mathrm{C_dA}$ values for all cold values are within 2% of the measured value from water calibration. Second, that the NOFB propellant was definitely flash boiling in the injectors, because the SPI method underpredicts the required $\mathrm{C_dA}$ at all temperatures. Third, that the injector face temperature has a significant effect on the required $\mathrm{C_dA}$, because the effective discharge area drops with increasing temperature. At 230°C the NHNE method underpredicts the $\mathrm{C_dA}$ by 25%, with the important caveat that these cal-

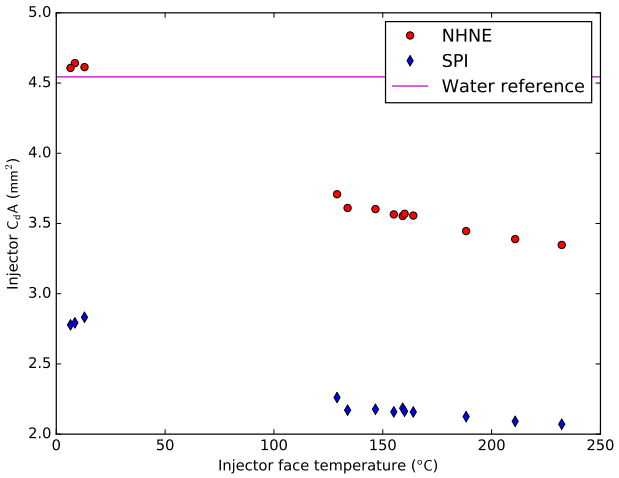

Figure 10: Effective discharge areas for the monopropellant injectors, plotted against the injector face temperature.

culations are using the propellant temperature in the premix chamber, rather than directly before the injector face. Further propellant injection temperature data is therefore required to validate the NHNE method for hot firings ([10] only has cold flows).

5. CONCLUSIONS

This study successfully hot-fired a NOFB in liquid form, and the resulting combustion was stable and with good combustion efficiency at the desired operating condition of O/F 3.20. Despite the volatile nature of this propellant and unknown characteristics, the test programme was conducted safely with no flashback or detonation events seen. However, the desired number of tests could not be completed because the injector was damaged by unexpectedly high heat flux.

The NOFB was shown to have several pecularities because it is pre-mixed and therefore burns extremely close to the injector face: first, it loses a significant proportion of heat to the chamber walls, second, it has high injector face heat flux, and third, this high injector heat flux leads to more flash-boiling in the injectors.

Flashback was not seen with the liquid (pressurised) NOFB showerhead injector and nitrogen purge on shutdown. For more realistic thruster geometries, further work should concentrate on flashback arrestors and injector geometries suitable for NOFB in both the liquid and gaseous phases.

REFERENCES

[1] Mungas, G., et al. (2011). NOFBX Monopropulsion Overview, *14th Annual FAA Commercial Space Transportation Conference*.

[2] Kjell, A., & Crowe, B. (2016). Concluding a 5 year in-space demonstration of an ADN-based propulsion system on PRISMA, *Space Propulsion Conference*, Rome

[3] Spores, R., et al. (2013). GPIM AF-M315E Propulsion system, *50th AIAA/SAE/ASEE Joint Propulsion Conference*, Ohio.

[4] Perakis, N., et al. (2014). Development of an experimental demonstrator unit using Nitrous Oxide / Ethylene pre-mixed Bipropellant for satellite applications Development at DLR, *Meet the space conference*, Krakow.

[5] Werling, L. and Perakis, N. (2016). Hot firing of a N2O / C2H4 pre-mixed green propellant. First combustion tests and results, *Space Propulsion Conference*, Rome.

[6] Werling, L., et al. (2016). Pressure Drop Measurement of Porous Materials; Flashback Arrestors for a N2O/C2H4 pre-mixed Green Propellant, *52nd AIAA/SAE/ASEE Joint Propulsion Conference*, Atlanta, GA.

[7] Perakis, N., et al. (2016). Numerical calculation of heat flux profiles in a N2O/CH2H4 pre-mixed green propellant combustor using an inverse heat conduction method, *Space Propulsion Conference*, Rome.

[8] Werling et al. (2017). Experimental Performance Analysis (c^* and c^* efficiency) of a pre-mixed green propellant consisting of N2O and C2H4, *53rd AIAA/SAE/ASEE Joint Propulsion Conference*.

[9] Mayer, A., et al. (2018). European Fuel Blend Development for space craft propulsion, *Space Propulsion Conference*, Seville.

[10] Waxman, B., et al. (2013). Mass flow rate and isolation characteristics of injectors for use with self-pressurizing oxidizers in hybrid rockets, *49th AIAA/ASME/SAE/ASEE Joint Propulsion Conference*, San Jose, CA.

[11] Dyer, J., et al. (2007). Modeling Feed System Flow Physics for Self-Pressurizing Propellants, *43rd AIAA/ASME/SAE/ASEE Joint Propulsion Conference and Exhibit*, Cincinnati, OH.

[12] Solomon, B. (2011). Engineering Model to Calculate Mass Flow Rate of a Two-Phase Saturated Fluid Through An Injector Orifice, Utah State University.

[13] McBride, B., & Gordon, S. (1996). Computer Program for Calculation of Complex Chemical Equlibrium Compositions and Applications, NASA RP1311.

[14] Deeken, J. et al. (2011). Combustion efficiency of a porous injector during throttling of a LOX/H2 combustion chamber, *Progress in Propulsion Physics*, 2011 (2).